  Bull. Chem. Soc. Jpn., 61, 3417—3420 (1988)

Evaluation of Kinetic Parameters from Steady-State Voltammograms at Ultramicrodisk Electrodes

Takayuki ABE, Kingo ITAYA,* Isamu UCHIDA, Koichi AOKI,† and Koichi TOKUDA†
Department of Applied Chemistry, Faculty of Engineering, Tohoku University, Aoba, Aramaki, Sendai 980
†Department of Electronic Chemistry, Graduate School at Nagatsuta, Tokyo Institute of Technology, Nagatsuta, Midori-ku, Yokohama 227
(Received March 29, 1988)

Platinum ultramicrodisk electrodes 0.8 μm in radius were constructed by anodic electropolishing of a platinum wire followed by sealing it with soft glass. Voltammograms for oxidation of $[Mo(CN)_8]^{4-}$, Fe^{2-}, and $[Fe(CN)_6]^{4-}$, being of a sigmoidal form, were measured at these electrodes and microdisk electrodes with 7.5 μm in radius under the essentially steady-state condition. A voltammogram of Fe^{2+} at 7.5 μm electrode was drawn out, exhibiting a halfwave potential shifted from the formal potential. This trend was more distinctive for a wave at 0.8 μm electrode. Radii of the electrodes and diffusion coefficients of the electroactive species were determined consistently from the limiting currents. The conventional log-plot showed that electrode reactions of Fe^{2+} and $[Fe(CN)_6]^{4-}$ were, respectively, totally irreversible and almost reversible at these electrodes. Application of the modified log-plot to the voltammograms yielded straight line, of which slope allowed us to evaluate the transfer coefficient and of which intercept gave values of the charge-transfer rate constant. Simulated voltammograms at these values were in good agreement with experimental ones.

Since mass transport at ultramicroelectrodes is caused by two- or three-dimensional diffusion rather than linear diffusion, the diffusional flux at ultramicroelectrodes is larger than that at electrodes on a conventional scale. This trend becomes remarkable as electrolysis time is long. For example, the ratio of the diffusional flux at a microdisk electrode 10 μm in diameter to that at conventional electrodes is 5.3, 11, and 46, respectively, at 0.1, 1, and 10 s.[1] Thus overall electrode reactions at ultramicroelectrodes are often complicated by charge-transfer kinetics even at a long time electrolysis. Investigations on the charge-transfer kinetics have been undertaken at very small mercury droplets on a vitreous carbon electrode,[2] microring electrodes,[3-5] microdisk electrodes,[6-10] microcylinder electrodes[11-16] and at microband electrodes.[17,18] Since measurements of voltammograms at these electrodes can be made under the quasi-steady state or the steady-state conditions, they are free from complication associated with current transient.

The microdisk electrode makes the kinetic effect most distinctive of the ultramicroelectrodes currently employed. This intriguing feature encouraged derivation of analytical equations for stationary voltammograms complicated by the electrode kinetics at the microdisk electrode.[9] According to the theory,[9] the voltammogram can be transformed into a linear curve through a modified log-plot, of which slope and intercept provide kinetic parameters. In order to apply the modified log-plot to experimental curves, it is required to confirm the establishment of the steady state, to establish a method of residual current elimination or correction and to determine consistently the radius of the electrode and diffusion coefficients. In the paper, we construct platinum ultramicrodisk electrodes by anodic electropolishing[19,20] and measure stationary voltammograms for oxidation of Fe^{2+} and $[Fe(CN)_6]^{4-}$. From these curves, we evaluate the kinetic parameters by use of the modified log-plot, aiming at verification of the theory.

Experimental

Microdisk Electrodes. Two kinds of microdisk electrodes were constructed, one being ca. 7.5 μm in radius and the other being less than 1 μm. A platinum wire 7.5 μm in radius and 2 mm in length (Tanaka Noble Metal Ltd., Tokyo) was connected electrically to a copper wire with mercury contact. It was sealed with soft glass. The surface of the electrode was polished with 1200 mesh carbon powder on a glass plate until the disk-shaped electrode was exposed. It was polished with 0.05 μm alumina powder, followed by ultrasonication in distilled water for 5 minutes. A view of the exposed electrode through a SEM was a well-defined disk rather than a deformed circle.

An ultramicro filament with a radius less than 1 μm was constructed by anodic electropolishing of a platinum wire 32.5 μm in radius, according to a technique described previously.[19,20] The polished filament tapered off to a top. It was dipped into fused soft glass in a small furnace at 320 °C to yield a surface coating of soft glass with a few μm in thickness. This coating ensures high quality of the sealing. The coated filament was cured with epoxy resin (Quetol 812, Nisshin EM, Tokyo) and kept at 60 °C for 24 h. The epoxied block was cut with a diamond knife (Diatome) mounted with an ultramicrotome (Porter-BLUM Model MT2-B). It was difficult to discern quality of a circle through a SEM photograph. The shape was assumed to be a disk for the data analysis. Prior to each electrochemical msasurement, the electrode surface was renewed by the cutting; polished with 0.05 μm alumina powder, dipped into concentrated nitric acid for 2 min and rinsed with distilled water.

Electrochemical Measurements. Since Faradaic currents were as small as 10 nA, a two-electrode system was employed for current measurements, in which a saturated calomel electrode (SCE) was served as a counter electrode. Currents were measured with a high speed current amplifier (Keithley Model 427) in an electrically sealed box. An electrochemical cell was thermostated at 25 °C in a water bath. Before mea-

surements, the solution was deaerated with nitrogen gas for 20 min. All chemicals were of analytical grade.

Results and Discussion

We used oxidation of $[Fe(CN)_6]^{4-}$ and Fe^{2+} as a model reaction associated with electrode kinetics because these two species have well investigated electrochemically. Figure 1 shows three examples of background-corrected voltammograms for oxidation of $[Fe(CN)_6]^{4-}$ (Flg. 1A) and Fe^{2+} (Figs. 1B and 1C) at the potential sweep rate of 10 mV s^{-1}. Residual currents were almost a straight line, of which slope was ca. 0.8 nA V^{-1} for curves in Figs. 1A and 1B and 0.05 nA V^{-1} in Fig. 1C. Since they traced the same path at the forward and the reverse potential scan, they do not result from a capacitive factor. Thus, these electrodes are successful in excluding fully the capacitive current which frequently degrades voltammograms at microdisk electrodes. Hysteresis of the voltammogram was slight but sometimes detectable (in Fig. 1C). The current at the reverse scan was always smaller than the forward one. Two reasons for the hysteresis can be considered: One is unreached steady state and the other is deterioration of the electrode surface during electrolysis. We examined theoretically the extent of the unreached steady state through use of a geometrical parameter, $p=(nFa^2v/RTD)^{1/2}$, in linear sweep voltammetry, where a is a radius of the disk electrode, v the potential sweep rate, n the number of electrons transferred, F the faraday constant, R the gas constant, T the temperature, and D the diffusion coefficient.[21] Values of p were less than 0.21 for $a \leqq 7.5$ μm at $n=1$, $v=10$ mV s^{-1} and $D=0.5\times10^{-5}$ cm^2 s^{-1}, suggesting that the deviation from the steady-state current would be less than 3%[21] if the voltammogram were reversible. Thus the hysteresis is ascribed to deterioration of the electrode. When hysteresis was observed, voltammograms only at the forward scan were employed for the following data analysis.

Radii of the two kinds of microdisk electrodes were evaluated from measurements of the stationary diffusion-controlled limiting current, I_d, for oxidation of 5 mmol dm^{-3} $[Mo(CN)_8]^{4-}$ in 0.5 mol dm^{-3} Na_2SO_4 through the following equation:[22]

$$I_d = 4nFc^*Da \qquad (1)$$

where c^* is the bulk concentration of the electroactive species. It was assumed that $D=4.6\times10^{-6}$ cm^2 s^{-1} for $[Mo(CN)_8]^{4-}$.[19] The calculated value of the radius of the large electrode was identical with a nominal value; 7.5 μm. The evaluated radius of the electropolished electrode was 0.70 μm.

We attempted to evaluate the radii from the limiting currents in Fig. 1 by use of $D=4.7\times10^{-6}$ cm^2 s^{-1} for Fe^{2+}[23] and $D=6.32\times10^{-6}$ cm^2 s^{-1} for $[Fe(CN)_6]^{4-}$.[24] The radii were 7.5 and 7.1 μm, respectively, for curves in Figs. 1A ($[Fe(CN)_6]^{4-}$) and 1B (Fe^{2+}). The former is in good agreement with both the nominal value and

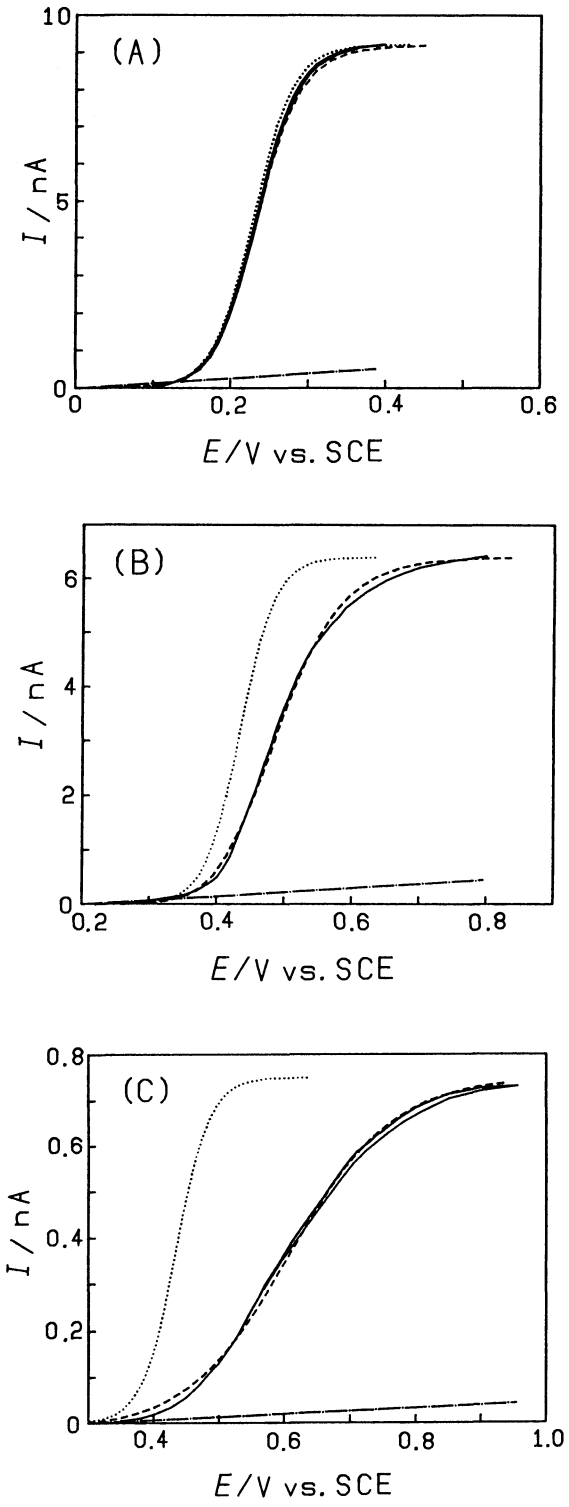

Fig. 1. Cyclic voltammogram (——) for 5 mmol dm^{-3} $[Fe(CN)_6]^{4-}$ in 1 mol dm^{-3} HCl solution at the electrode of $a=7.5$ μm (Fig. 1A), that (——) for 5 mmol dm^{-3} Fe^{2+} in 1 mol dm^{-3} H_2SO_4 solution at the electrode of $a=7.5$ μm (Fig. 1B) and that (——) for 5 mmol dm^{-3} Fe^{2+} in 1 mol dm^{-3} H_2SO_4 solution at the electrode of $a=0.88$ μm (Fig. 1C) when measure at $v=10$ mV s^{-1}. Curves (-·-·-) are residual currents. Dashed curves are simulated waves calculated from Eq. 5 at kinetic parameters evaluated from the modified log-plot. Reversible voltammograms might be expressed by dotted curves.

the value evaluated from the current of $[Mo(CN)_8]^{4-}$. Slight discrepancy for the latter may be due to an incomplete plateau of the limiting current. An expedient of satisfying Eq. 1 so as to make no influence on the log-plot is to determine the diffusion coefficient of Fe^{2+} specific to this electrochemical system. The value of D thus determined is 4.4×10^{-6} $cm^2 s^{-1}$. This value will be used for D of Fe^{2+} in the discussion below. On the other hand, the radius evaluated from the limiting current in Fig. 1C by use of the above value of D was 0.88 μm, which was larger than 0.70 μm evaluated for $[Mo(CN)_8]^{4-}$. Such difference was frequently observed when the electrode surface was renewed by cutting at each measurement. The discrepancy may not be ascribed to difference in electroactive species but may be attributed to poor reproducibility of the renewal. Thus, for the analysis of a voltammetric waveform, it is desirable to use a radius determined from a limiting current at each renewed electrode.

According to the theory of the stationary voltammogram involving electrode kinetics at microdisk electrodes, the current-potential curves for the quasi-reversible and the totally irreversible waves are expressed by the following modified log-plot:[9]

$$E=E^*-2.3\frac{RT}{(1-\alpha)nF}\log\frac{[1-(I/I_d)\{1+\exp(-nF(E-E^{\circ\prime})/RT)\}]^{1.11}}{I/I_d} \quad (2)$$

with

$$E^*=E^{\circ\prime}-2.3[RT/\{(1-\alpha)nF\}]\log[(\pi/4)k^{\circ\prime}a/D] \quad (3)$$

where the Butler-Volmer equation has been used for the kinetic equation. Here I is the current at electrode potential E, α the cathodic transfer coefficient, $k^{\circ\prime}$ is the formal electrode reaction rate constant, and $E^{\circ\prime}$ the formal potential. On the other hand, the reversible wave can simply be expressed by

$$E=E^{\circ\prime}+2.3(RT/nF)\log[I/(I_d-I)] \quad (4)$$

We temporarily assume that the voltammograms in Fig. 1 are reversible. The conventional log-plots given by Eq. 4 are shown in Fig. 2. Plot A for $[Fe(CN)_6]^{4-}$ falls on a straight line of which inverse slope is 62 mV. The half-wave potential is shifted positively by 3 mV from the middle value (0.230 V vs. SCE) of the anodic and the cathodic peak potential measured at a platinum disk electrode 2 mm in diameter. Thus the reaction is very close to the reversible one although there appears slight kinetic effects. On the other hand; plots B and C for Fe^{2+} are curved and half-wave potentials are positively shifted by 55 and 171 mV, respectively, from the middle value (0.435 V vs. SCE) of the anodic and the cathodic peak potential measured at the large electrode. Thus the oxidation of Fe^{2+} belongs to the totally irreversible group. The difference in the radius is obviously responsible for the difference in the participation of electrode kinetics. From the empirical concept on the electrode kinetics, logarithm of the reduced rate constant, $k^{\circ\prime}a/D$, has linear relation with $(1-\alpha)(nFE/RT)$. Thus the difference in the half-wave potential may be equivalent to $[RT/\{(1-\alpha)nF\}]\ln(a_B/a_C)$, where a_B and a_C are radii of electrodes for curves B and C, respectively. The difference in the measured half-wave potential was 0.116 V while the differences calculated from $\ln(a_B/a_C)$ were 0.110 and 0.117 V for $\alpha=0.5$ and $\alpha=0.53$, respectively. Agreement is good for reasonable values of α, demonstrating that miniaturizing electrodes causes the potential shift by the amount of $[RT/\{(1-\alpha)nF\}]\ln(a_0/a)$, where a_0 is the reference radius of a microdisk electrode.

It is possible to evaluate $k^{\circ\prime}$ and α from the modified log-plot through Eqs. 2 and 3. In Fig. 3, values of E are plotted against the logarithmic term involving Eq. 2 for the three voltammograms. Although plots B and C are slightly curved, the points fall on a straight line.

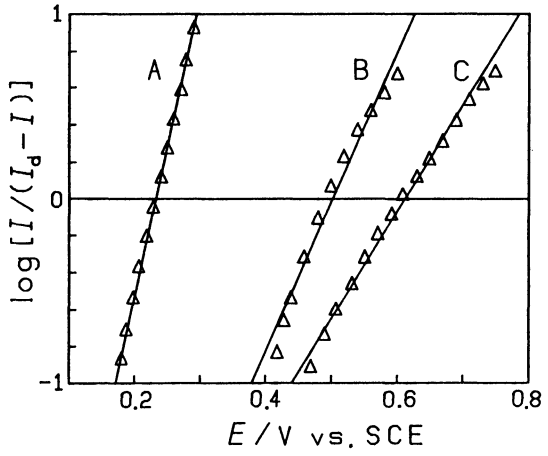

Fig. 2. Conventional log-plots for stationary voltammograms of (A) $[Fe(CN)_6]^{4-}$ at the electrode of $a=7.5\,\mu m$, (B) Fe^{2+} at $a=7.5\,\mu m$ and (C) Fe^{2+} at $a=0.88\,\mu m$. These three plots correspond to voltammograms in Fig. 1.

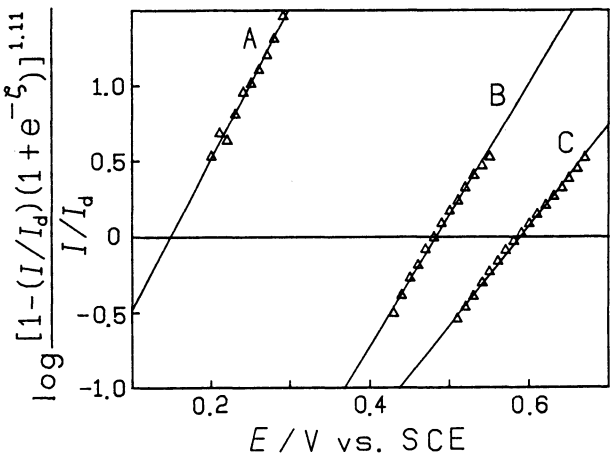

Fig. 3. Modified log-plots for voltammograms in Fig. 1. Plots A, B, and C correspond to waves in Fig. 1.

Equation 2 shows that the slope of the plot is $2.3RT/\{(1-\alpha)nF\}$, from which α can be evaluated. The slope was evaluated by the method of linear least squares. Values of α are 0.48 and 0.65 for plots B and C, respectively. The literature value is 0.58.[25] The intercept with the E-axis gives E^*, which determines $k^{o\prime}$ through Eq. 1 at known values of $E^{o\prime}$, α, and D. Values of $k^{o\prime}$ thus obtained are 3.0×10^{-3} (α=0.48, $D=4.4\times10^{-6}$ cm^2 s^{-1}, a=7.5 μm) and 6.5×10^{-3} cm s^{-1} (α=0.65, $D=4.4\times10^{-6}$ cm^2 s^{-1}, a=0.88 μm) for plots B and C, respectively. The discrepancy of $k^{o\prime}$ is ascribed to the difference in α because it has been demonstrated in the above that the difference in the half-wave potential was equivalent quantitatively to $\ln(k^{o\prime}a/D)$ at a common value of α. The difference in α may result in edge effects other than those due to diffusion, e.g., activation at the edge, selective adsorption at the edge, and deformation of the disk form of the electrode. If we take a common value of α to be 0.55 retaining values of E^*, values of $k^{o\prime}$ become common, being 3×10^{-3} cm s^{-1}.

Plot A in Fig. 3 falls on a straight line although the line is sensitive to errors in $E^{o\prime}$. The kinetic parameters from this straight line are α=0.43 and $k^{o\prime}$=0.07 cm s^{-1}. We attempted to measure voltammograms of $[Fe(CN)_6]^{4-}$ at an electrode with a radius less than 1 μm. Voltammograms were almost the same as in Fig. 1A, suggesting that the kinetic effect is vague. Consequently, $[Fe(CN)_6]^{4-}$ belongs to the reversible group rather than the quasi-reversible one at microelectrodes employed here. The kinetic values determined above may involve large errors.

We simulated the voltammograms through use of Eq. 2 for kinetic parameters obtained from the modified log-plot. Since Eq. 2 is non-linear with respect to both E and I, we valuated I/I_d at a given value of E through the following algorithm based on the Newton method:

$$x_{k+1}=x_k-f(x_k)/f'(x_k) \tag{5}$$

with

$$x_k=(I/I_d)_k$$
$$f(x)=[1-x\{1+\exp(-\zeta)\}]^{1.11}/x - \exp[-(1-\alpha)(nF/RT)(E-E^*)]$$
$$f'(x)=[1-x\{1+\exp(-\zeta)\}]^{0.11}[0.11\{1+\exp(-\zeta)\}x]/x^2$$
$$\zeta=(nF/RT)(E-E^{o\prime})$$

Starting at an initial value, x_0, less than $\exp[(1-\alpha)(nF/RT)(E-E^*)]$, we could successfully computed converged values of I/I_d. Values for the parameters employed for the simulation are $k^{o\prime}$=0.07 cm s^{-1}, α=0.43, $D=6.32\times10^{-6}$ cm^2 s^{-1}, a=7.5 μm for curve A, $k^{o\prime}=3.0\times10^{-3}$ cm s^{-1}, α=0.48, $D=4.4\times10^{-6}$ cm^2 s^{-1}, a=7.5 μm for curve B, $k^{o\prime}=6.5\times10^{-3}$ cm s^{-1}, α=0.65, $D=4.4\times10^{-6}$ cm^2 s^{-1}, a=0.88 μm for curve C. In Fig 1, simulated curves (---) are drawn, in good agreement with experimental waves. This fact indicates that the kinetic parameters obtained here are reasonable although there is no consistency in the kinetic parameters for curves B and C.

References

1) K. Aoki and J. Osteryoung, *J. Electroanal. Chem.*, **169**, 335 (1984).
2) P. Bindra, A. P. Brown, M. Fleischmann, and D. Pletcher, *J. Electroanal. Chem.*, **58**, 31 (1975); **58**, 39 (1975).
3) M. Fleischmann, J. Ghoroghchian, and S. Pons, *J. Phys. Chem.*, **89**, 5530 (1985).
4) A. Russell, K. Repka, T. Dibble, J. Ghoroghchian, J. J. Smith, M. Fleischmann, C. H. Pitt, and S. Pons, *Anal. Chem.*, **58**, 2961 (1986).
5) A. Szabo, *J. Phys. Chem.*, **91**, 3108 (1987).
6) B. Scharifker and G. Hills, *J. Electroanal. Chem.*, **130**, 81 (1981).
7) G. Hills, A. K. Pour, and B. Scharifker, *Electrochim. Acta*, **28**, 891 (1983).
8) J. O. Howell and R. M. Wightman, *Anal. Chem.*, **56**, 524 (1984).
9) K. Aoki, K. Tokuda, and H. Matsuda, *J. Electroanal. Chem.*, **235**, 87 (1987).
10) M. I. Montenegro and D. Pletcher, *J. Electroanal. Chem.*, **200**, 371 (1986).
11) K. Aoki, K. Tokuda, and H. Matsuda, *J. Electroanal. Chem.*, **206**, 47 (1986).
12) K. Aoki, K. Tokuda, and H. Matsuda, *J. Electroanal. Chem.*, **175**, 1 (1984).
13) M. R. Deakin, *J. Electrochem. Soc.*, **132**, 496C (1985).
14) C. A. Amatore, M. R. Deakin, and R. M. Wightman, *J. Electroanal. Chem*, **206**, 23 (1986).
15) K. Aoki and H. Kaneko, *J. Electroanal. Chem.*, **247**, 17 (1988).
16) K. Aoki, H. Kaneko, and K. Nozaki, *J. Electroanal. Chem.*, **247**, 29 (1988).
17) M. R. Reakin, R. M. Wightman, and C. A. Amatore, *J. Electroanal. Chem.*, **215**, 49 (1986).
18) C. A. Amatore, B. Fosset, M. R. Deakin, and R. M. Wightman, *J. Electroanal. Chem.*, **225**, 33 (1987).
19) K. Itaya, T. Abe, and I. Uchida, *J. Electrochem. Soc.*, **134**, 1191 (1987).
20) T. Abe, K. Itaya, and I. Uchida, *Chem. Lett.*, in press.
21) K. Aoki, K. Akimoto, K. Tokuda, H. Matsuda, and J. Osteryoung, *J. Electroanal. Chem.*, **171**, 219 (1984).
22) K. Aoki and J. Osteryoung, *J. Electroanal. Chem.*, **215**, 49 (1986).
23) H. P. Agarwal and S. Qureshi, *Electrochim. Acta*, **19**, 607 (1974).
24) M. V. Stackelberg and V. Toome, *Z. Elektrochem.*, **58**, 226 (1954).
25) H. P. Agarwal, *J. Electroanal. Chem.*, **5**, 236 (1963).